Langmuir Article

pubs.acs.org/Langmuir

Influence of Lipids on the Interfacial Disposition of Respiratory Syncytical Virus Matrix Protein

Helen K. McPhee,[†] Jennifer L. Carlisle,[†] Andrew Beeby,[†] Victoria A. Money,[†] Scott M. D. Watson,[†] R. Paul Yeo,*[,‡] and John M. Sanderson*[,†]

[†]*Department of Chemistry and Biophysical Sciences Institute, Durham University, South Road, Durham DH1 3LE, United Kingdom, and* [‡]*School for Medicine and Health, Queen's Campus, Durham University, Stockton-on-Tees TS17 6BH, United Kingdom*

Received October 7, 2010. Revised Manuscript Received November 22, 2010

The propensity of a matrix protein from an enveloped virus of the *Mononegavirales* family to associate with lipids representative of the viral envelope has been determined using label-free methods, including tensiometry and Brewster angle microscopy on lipid films at the air−water interface and atomic force microscopy on monolayers transferred to OTS-treated silicon wafers. This has enabled factors that influence the disposition of the protein with respect to the lipid interface to be characterized. In the absence of sphingomyelin, respiratory syncytial virus matrix protein penetrates monolayers composed of mixtures of phosphocholines with phosphoethanolamines or cholesterol at the air−water interface. In ternary mixtures composed of sphingomyelin, 1,2-dioleoyl-*sn*-glycero-3-phosphocholine, and cholesterol, the protein exhibits two separate behaviors: (1) peripheral association with the surface of sphingomyelin-rich domains and (2) penetration of sphingomyelin-poor domains. Prolonged incubation of the protein with mixtures of phosphocholines and phosphoethanolamines leads to the formation of helical protein assemblies of uniform diameter that demonstrate an inherent propensity of the protein to assemble into a filamentous form.

Introduction

A significant number of human viral pathogens (e.g., ebola, measles, rabies, human immunodeficiency virus, influenza) are characterized by the presence of an outer envelope. These envelopes comprise a phospholipid bilayer that is acquired from cellular membranes by budding. In order to achieve virion assembly and budding, there must be a coordinated accumulation of viral components in specific cellular membrane regions, which is reflected in the lipid composition of the envelope. However, although the lipid composition of the viral envelope is known in some cases, the distributions of lipids within these membranes, and the key protein interactions that drive virion morphology, are poorly understood. Key interactions between some viral proteins and the membrane are a fundamental feature of virion formation. A number of proteins are intimately associated with the envelope, including glycoproteins essential for viral entry into the host and proteins with key structural roles. Examples of the latter include the matrix (M) proteins from the *Mononegavirales*, peripheral membrane proteins with key roles in determining virion morphology and driving the budding process.[1−4] Despite the similar roles played by matrix proteins from all *Mononegavirales* families, there are nevertheless morphological differences between their virions, with some exhibiting a filamentous shape (*Filoviridae*) or a bullet shape (*Rhabdoviridae*), while others are pleiomorphic (*Paramyxoviridae*). Respiratory syncytial virus (RSV) is an example of the latter, exhibiting both spherical and filamentous morphologies.[5] Filaments, in particular, are imaged as processes that extend from the cell in a similar manner to filopodia and are associated with viral proteins. Filaments are assumed to be the sites of viral budding,[6] making the underlying factors that control filament formation of fundamental importance for our understanding of virion morphogenesis.

A number of studies have implicated a role for lipid microdomains (often termed "rafts")[7−11] in the assembly and budding processes.[12−15] These assertions are frequently made following isolation of viral proteins from detergent-resistant membrane fractions (DRMs).[6,16−19] Notably, RSV assembles in regions of the host cell membrane which are rich in lipids that are associated with microdomain formation *in vitro*.[20] The RSV M and surface glycoproteins colocalize with these lipids.[6] In addition, viral envelopes contain phosphocholines, phosphoethanolamines,

*To whom correspondence should be addressed. E-mail: j.m.sanderson@durham.ac.uk. Tel: +44 (0)191 3342107. Fax: +44 (0)191 3844737.

(1) Collins, P. L.; Chanock, R. M.; Murphy, B. R. In *Fields Virology*; Knipe, D. M., Howley, P. M., Griffin, D. E., Lamb, R. A., Martin, M. A., Roizman, B., Straus, S. E., Eds.; Lippincott-Raven: Philadelphia, 2001; Vol. *1*, pp 1443−1486.
(2) Murphy, L. B.; Loney, C.; Murray, L.; Bhella, D.; Ashton, P.; Yeo, R. P. *Virology* **2003**, *307*, 143–153.
(3) Lamb, R. A.; Kolakofsky, D. In *Fields Virology*; Knipe, D. M., Howley, P. M., Griffin, D. E., Lamb, R. A., Martin, M. A., Roizman, B., Straus, S. E., Eds.; Lippincott-Raven: Philadelphia, 2001; Vol. *1*.
(4) Fuentes, S.; Tran, K. C.; Luthra, P.; Teng, M. N.; He, B. *J. Virol.* **2007**, *81*, 8361–8366.
(5) Bächi, T.; Howe, C. *J. Virol.* **1973**, *12*, 1173–1180.
(6) Henderson, G.; Murray, J.; Yeo, R. P. *Virology* **2002**, *300*, 244–254.
(7) London, E.; Brown, D. A. *Biochim. Biophys. Acta* **2000**, *1508*, 182–195.
(8) Marsh, D. *Biochim. Biophys. Acta* **2008**, *1778*, 1545–1575.
(9) Simons, K.; Vaz, W. L. C. *Annu. Rev. Biophys. Biomol. Struct.* **2004**, *33*, 269–295.
(10) Sengupta, P.; Baird, B.; Holowka, D. *Semin. Cell Dev. Biol.* **2007**, *18*, 583–590.
(11) Silvius, J. R. *Biochim. Biophys. Acta* **2005**, *1746*, 193–202.
(12) Chazal, N.; Gerlier, D. *Microbiol. Mol. Biol. Rev.* **2003**, *67*, 226–237.
(13) Brown, G.; Jeffree, C. E.; McDonald, T.; Rixon, H. W. M.; Aitken, J. D.; Sugrue, R. J. *Virology* **2004**, *327*, 175–185.
(14) Marty, A.; Meanger, J.; Mills, J.; Shields, B.; Ghildyal, R. *Arch. Virol.* **2004**, *149*, 199–210.
(15) Laliberte, J. P.; McGinnes, L. W.; Peeples, M. E.; Morrison, T. G. *J. Virol.* **2006**, *80*, 10652–10662.
(16) Manié, S. N.; Debreyne, S.; Vincent, S.; Gerlier, D. *J. Virol.* **2000**, *74*, 305–311.
(17) Pohl, C.; Duprex, W. P.; Krohne, G.; Rima, B. K.; Schneider-Schaulies, S. *J. Gen. Virol.* **2007**, *88*, 1243–1250.
(18) Bavari, S.; Bosio, C. M.; Wiegand, E.; Ruthel, G.; Will, A. B.; Geisbert, T. W.; Hevey, M.; Schmaljohn, C.; Schmaljohn, A.; Aman, M. J. *J. Exp. Med.* **2002**, *195*, 593–602.
(19) Ali, A.; Nayak, D. P. *Virology* **2000**, *276*, 289–303.
(20) Brown, G.; Rixon, H. W. M.; Sugrue, R. J. *J. Gen. Virol.* **2002**, *83*, 1841–1850.

cholesterol, and sphingomyelins as major components.[21] However, the correlation between the compositions of lipid microdomains and DRMs is the subject of debate.[8,22−25] There is particular concern that the addition of detergents during DRM isolation unduly influences the mixing behavior of complex lipid systems, leading to the presence of components that do not reflect the lipid distribution *in vivo*. In model membranes, lateral phase separation to form microdomains is promoted by the presence of cholesterol. Microdomains, consisting of solid-ordered (s_0) or liquid-ordered (l_0) regions rich in cholesterol and saturated lipids, are characterized by a high lipid packing density and low fluidity relative to the remainder of the membrane, which resides in a more fluid liquid-disordered (l_d) state.[22] Although the presence of l_0 domains is well established *in vitro* in ternary lipid mixtures such as 1,2-dioleoyl-*sn*-glycero-3-phosphocholine (DOPC)/1,2-palmitoyl-*sn*-glycero-3-phosphocholine (DPPC)/cholesterol[26−28] and DOPC/sphingomyelin (SM)/cholesterol,[27,29,30] their presence is less well characterized *in vivo*.[31,32]

Considering the arguments above, experiments with model membrane mixtures that exhibit microphase separation and are representative of the viral envelope are attractive as a means of understanding the partitioning behavior of these membrane proteins. As the X-ray crystal structure of the M protein from RSV has recently been described,[33] this is an ideal target for examining whether matrix proteins have an inherent ability to associate with particular lipids in model systems and examine whether particular lipid compositions are able to promote polymorphism of matrix protein assembly.

Experimental Section

General. All work was conducted in phosphate-buffered saline (PBS) at pH 7.4 and a temperature of 20 °C. RSV M protein bearing a single point substitution (M254 to R) was used for binding experiments, prepared as described previously.[33] All lipids and cholesterol were obtained as pure solids from either Bachem AG (Bubendorf, Switzerland), Alfa Aesar (Heysham, Lancashire, UK), or Sigma-Aldrich Ltd. (Dorset, UK). SM from egg yolk was obtained from Fluka (Dorset, UK). Matrix protein samples were stored at 4 °C and used in PBS at pH 7.4. Prior to each experiment, the protein sample was centrifuged at 100000*g* for 30 min at 4 °C to remove nucleation centers and the protein concentration redetermined.

Tensiometry. A dual-barrier Langmuir trough (102M, Nima Technology Ltd., Coventry, UK) was used for all tensiometry. Lipid films were spread in chloroform, equilibrated for 15−20 min, and subjected to three cycles of half-compression/expansion. The final isotherm was recorded at a barrier speed of 9 $cm^2\ min^{-1}$. For isotherms with RSV M, the protein was added to the surface prior to the spreading of the lipid. The surface pressure, Π, was

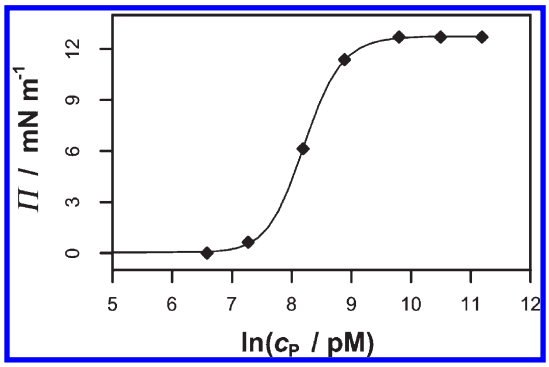

Figure 1. Adsorption isotherm at the air−water interface for RSV M protein in PBS at pH 7.4, 20 °C. Points (filled diamonds) correspond to experimental values, with the calculated curve (Π_c) from fitting of eqs 2 and 3 (see Experimental Section) represented as a line.

calculated from the surface tension, γ, according to eq 1:

$$\Pi = \gamma_0 - \gamma \quad (1)$$

where γ_0 is the observed surface tension at the air−water interface in the absence of protein or lipid.

Protein Suface Activity. For protein adsorption isotherms, the surface tension data were modeled using a four-parameter logistic equation[34]

$$\gamma_c = \left(\frac{\gamma_w - \gamma_l}{1 + (\ln c_P^{\Pi/2}/\ln c_P)^B}\right) + \gamma_l \quad (2)$$

where γ_c is the calculated interfacial tension, γ_w and γ_l are the horizontal asymptotes, $c_P^{\Pi/2}$ is the protein concentration for half-maximal change in interfacial tension, and B is a factor that describes the gradient of the linear part of the curve. The limiting surface pressure Π^{max} (i.e., $\gamma_w - \gamma_l$) was determined from the fitted parameters. Although nonlinear least-squares fitting was conducted using eq 2, the data are more conveniently presented (as for the solid line in Figure 1) in terms of surface pressure, calculated according to eq 3:

$$\Pi_c = \gamma_w - \gamma_c \quad (3)$$

where Π_c is the calculated surface pressure.

The apparent Gibbs surface excess (Γ_a) was determined from the gradient of the linear part of the sigmoidal curve (eq 4)[35,36] and the concentration required to produce the maximum change in interfacial tension (c_P^{max}) obtained by extrapolation of the linear part of the curve to $\gamma = \gamma_l$.

$$\Gamma_a = \frac{1}{RT}\frac{d\Pi}{d \ln c_P} \quad (4)$$

Preparation and Imaging of Protein−Lipid Films. Clean silicon (111) wafers were treated with a 1 mM solution of octadecytrichlorosilane (OTS) in dry toluene for 36 h. The wafers were sonicated successively in toluene and chloroform (each 2 × 15 min), before a final rinse with Milli-Q water. Protein−lipid films were spread on a PBS subphase in a Teflon dipping trough. The OTS-coated wafer was dipped downward through each film at constant pressure and released into a clean sample vial. Glutaraldehyde (2.6 M in water) was added to a final concentration of 250 mM. After 2 min, sodium borohydride (1 M solution in 0.2 M NaOH, 0.14 mol equiv with respect to glutaraldehyde) was added. AFM imaging was carried out in tapping mode using

(21) Gunstone, F. D.; Harwood, J. L. In *The Lipid Handbook*; Gunstone, F. D., Harwood, J. L., Dijkstra, A. J., Eds.; Chapman & Hall/CRC Press: London, 2007; p 141.
(22) Lichtenberg, D.; Goni, F. M.; Heerklotz, H. *Trends Biochem. Sci.* **2005**, *30*, 430–436.
(23) Heerklotz, H. *Biophys. J.* **2002**, *83*, 2693–2701.
(24) Brown, D. A. *Physiology* **2006**, *21*, 430–439.
(25) Garner, A. E.; Smith, D. A.; Hooper, N. M. *Biophys. J.* **2008**, *94*, 1326–1340.
(26) Veatch, S. L.; Polozov, I. V.; Gawrisch, K.; Keller, S. L. *Biophys. J.* **2004**, *86*, 2910–2922.
(27) Veatch, S. L.; Keller, S. L. *Phys. Rev. Lett.* **2005**, *94*, 148101−1–148101−4.
(28) Ahmed, S. N.; Brown, D. A.; London, E. *Biochemistry* **1997**, *36*, 10944–10953.
(29) Dietrich, C.; Bagatolli, L. A.; Volovyk, Z. N.; Thompson, N. L.; Levi, M.; Jacobson, K.; Gratton, E. *Biophys. J.* **2001**, *80*, 1417–1428.
(30) Samsonov, A. V.; Mihalyov, I.; Cohen, F. S. *Biophys. J.* **2001**, *81*, 1486–1500.
(31) Duggan, J.; Jamal, G.; Tilley, M.; Davis, B.; McKenzie, G.; Vere, K.; Somekh, M. G.; O'Shea, P.; Harris, H. *Eur. Biophys. J.* **2008**, *37*, 1279–1289.
(32) Edidin, M. *Annu. Rev. Biophys. Biomol. Struct.* **2003**, *32*, 257–283.
(33) Money, V. A.; McPhee, H. K.; Mosely, J. A.; Sanderson, J. M.; Yeo, R. P. *Proc. Natl. Acad. Sci. U.S.A.* **2009**, *106*, 4441–4446.
(34) Krishnan, A.; Siedlecki, C. A.; Vogler, E. A. *Langmuir* **2003**, *19*, 10342–10352.
(35) Seelig, A.; Gottschlich, R.; Devant, R. M. *Proc. Natl. Acad. Sci. U.S.A.* **1994**, *91*, 68–72.
(36) Seelig, A. *Biochemistry* **1992**, *31*, 2897–2904.

etched silicon probes with a spring constant of 40 N/m and a drive frequency of 300 kHz. Images were recorded at typical scan rates of 0.5−1.0 Hz with 256 scan lines. Images were analyzed using Nanoscope version 6.1.3 software (Veeco Instruments Inc., San Clemente, CA). Root-mean-square roughness (R_q) and average roughness (R_a) values were determined on scans of size 5 μm × 5 μm in all cases.

Brewster Angle Microscopy. Light from a p-polarized 633 nm helium−neon laser (CVI Melles-Griot, Leicester, UK) was passed through a Glan-Taylor polarizer and adjusted so that the beam was incident on the film surface in a dual-barrier Langmuir trough at an angle of ∼53° to the normal; the angle was adjusted until a minimal reflection was observed from a clean liquid surface. Reflected light was collected using a CCD video camera (Optem Zoom 70, Qioptik Imaging Solutions, Newport, NY) and digitized using LabView (National Instruments Corp., Austin, TX).

Formation of Protein Assemblies. A lipid film on the side of a glass vessel was rehydrated with a suitable volume of protein in PBS. The resulting suspensions was incubated at 37 °C for 5−7 days, followed by 2 days at 4 °C. Samples were examined by transmission electron microscopy (TEM) using a Hitachi TEM-H7600 transmission electron microscope (Hitachi, Maidenhead, UK), with an accelerating voltage of 80−100 kV.

Results and Discussion

Surface Adsorption of M. In order to determine the surface activity of the RSV M at the air−water interface, a surface adsorption isotherm was generated by measurement of the surface pressure (Π, eq 1) of solutions of the protein in phosphate buffered saline (PBS) as a function of the bulk protein concentration (c_P). Cross-linking studies on RSV M have identified oligomeric forms of the protein (dimer, tetramer, and hexamer) in solution.[33] However, at the protein concentrations used in these cross-linking experiments (10^{-5} M), the dimeric form was the dominant species, with a significant proportion of monomer remaining in spite of the perturbation of the equilibrium toward higher order oligomers as a result of cross-linking. Given that the RSV M concentration required for saturation of the air−water interface (Figure 1) is 4 orders of magnitude lower than that used for cross-linking, the monomeric form of the protein will be predominant in solution. In common with many proteins,[34,37] the surface pressure exhibited a sigmoidal dependency on the logarithm of c_P (Figure 1). Modeling the data (eqs 2 and 3) gave a limiting surface pressure (Π^{max}) of 12.7 ± 1.3 mN m^{-1}, with saturation of the surface occurring at a protein concentration ($c_P{}^{max}$) of 7.1 nM. This low surface pressure is indicative of a weak surface activity, consistent with preliminary data reported for another matrix protein.[38] The Gibbs adsorption equation (eq 4) was applied to calculate an apparent surface excess (Γ_a) for the protein of 4.2 ± 0.5 pmol cm^{-2}, corresponding to an area per molecule of 39.5 nm^2.

Although this is an "apparent" value, as it assumes that the activity coefficient of the protein is unaffected by ionization or conformational changes or the presence of other electrolytes,[34] it nevertheless gives an indication of the proportion of the surface of the protein that contributes to interfacial activity. The structures of both the native protein (Figure S3, Supporting Information) and the protein bearing a single point mutation[33] are characterized by two folded domains separated by a short unstructured linker. Taken independently, the dimensions of each domain are approximately 20 Å × 40 Å at the widest points, giving an maximal cross-sectional area for each of 8 nm^2. Even considering that the protein may be partially unfolded in the adsorbed state, and allowing for a significant difference between the true and apparent surface excesses, the value of 39.5 nm^2 per molecule indicates that both domains of the protein reside at least partially at the interface.

Adsorption of M to Lipid Monolayers. Pressure−area (Π−A) isotherms were obtained for thin films of lipids spread over PBS subphases containing RSV M protein over a range of concentrations (c_P). Lipids selected for investigation included a single-component phosphocholine (DOPC), mixtures of DOPC with DPPE, as phosphoethanolamines are a key viral membrane component with potential involvement in budding through the promotion of negative membrane curvature, and ternary mixtures of DOPC with cholesterol and either DPPC or sphingomyelin. The latter mixtures were used at 1:1:1 ratios, as separation into l_0 and l_d phases has been documented at these ratios for the temperatures used in tensiometry experiments,[26−30] enabling protein interaction with these phases to be assessed. For each lipid or lipid mixture, protein adsorption produced significant changes to the Π−A isotherms, necessitating careful optimization of the lipid concentration (c_L) in each case in order to enable data to be obtained over a range of Π−A values that included the monolayer−bilayer equivalence pressure,[39] the lift-off area for the lipid, film collapse in the presence of protein, and protein saturation of the interface. Because of differences in protein partitioning and Π−A behavior, the optimum lipid concentration was different for each case. Data for four lipid systems, each at an optimum fixed lipid concentration, are presented in Figure 2.

Two key features were apparent from the Π−A isotherms of thin films of DOPC (Figure 2a). First, for c_P < 8 nM, when compared with the lipid-only isotherm, significant increases in both pressure and area per lipid molecule were found in the presence of protein, indicating that the protein penetrates the monolayer. Second, saturation of the interface with the protein adsorbate occurred, with higher protein concentrations ($c_P \geq 8$ nM) producing no further modifications to the Π−A isotherm. For $c_P \geq$ 8 nM, collapse of the film was apparent at a surface pressure of 60 mN m^{-1}. The lipid molecular area at the onset of collapse shifted to higher areas with increasing c_P, again demonstrating that protein adsorption at the interface and penetration of the monolayer was occurring. A cross section through the isotherms at a constant area of 280 Å^2 per lipid molecule was used to obtain pressure−concentration data that were used to estimate an adsorption equilibrium constant for the protein, K, by fitting a modified Langmuir binding isotherm to the data. This gave a value for K of 2×10^8 M^{-1}, with an error of ±10% (Figure S4), indicative of a significant protein affinity for the interface. For monolayers composed of DOPC/DPPC/cholesterol (1:1:1), similar behavior to the DOPC monolayer was found in the presence of RSV M (Figure 2b), with protein penetration and film collpase at 60−65 mN m^{-1}. However, in this case saturation adsorption occurred at a lower bulk protein concentration ($c_P \approx 5$ nM), with a value for K of 8×10^8 M^{-1}, reflecting a higher protein affinity for the interface than observed with DOPC monolayers. A similar penetrative behavior and higher interfacial activity (compared to DOPC) was also found with monolayers of DOPC/DPPE (4:1) (Figure 2c; $K = 4 \times 10^8$ M^{-1} ± 10%).

Monolayers composed of DOPC/SM/cholesterol (1:1:1) produced strikingly different isotherms to the other lipid mixtures in the presence of RSV M protein (Figure 2d). From these isotherms, three different behaviors were distinguishable according

(37) Niño, R. R.; Sánchez, C. C.; Fernández, M. C.; Patino, J. M. R. *J. Am. Oil Chem. Soc.* **2001**, *78*, 873–879.
(38) Neumann, P.; Lieber, D.; Meyer, S.; Dautel, P.; Kerth, A.; Kraus, I.; Garten, W.; Stubbs, M. T. *Proc. Natl. Acad. Sci. U.S.A.* **2009**, *106*, 3710–3715.
(39) Marsh, D. *Biochim. Biophys. Acta* **1996**, *1286*, 183–223.

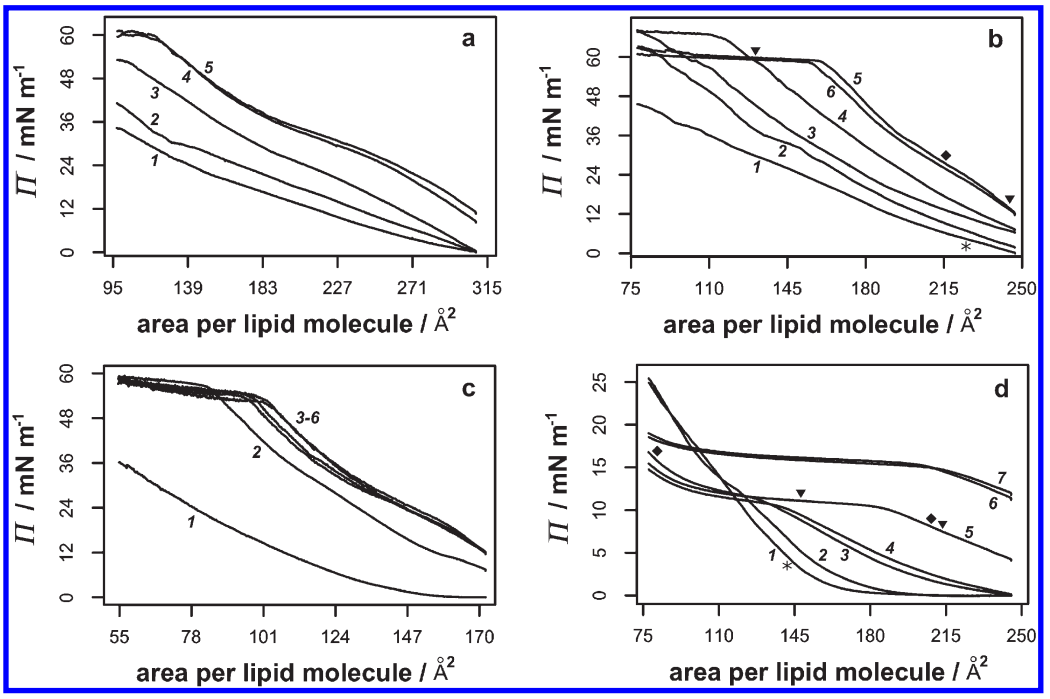

Figure 2. Pressure−area (Π−*A*) isotherms for lipid monolayers spread over a PBS subphase containing RSV M protein at 20 °C, pH 7.4: (a) DOPC, c_L = 165 nM; c_P/nM = 0 (**1**), 0.8 (**2**), 1.6 (**3**), 8.2 (**4**), 16.5 (**5**). (b) DOPC/DPPC/cholesterol (1:1:1), c_L = 117 nM; c_P/nM = 0 (**1**), 0.2 (**2**), 0.9 (**3**), 2.3 (**4**), 5.8 (**5**), 11.7 (**6**). (c) DPPE/DOPC (1:4), c_L = 169 nM; c_P/nM = 0 (**1**), 3.4 (**2**), 16.9 (**3**), 33.8 (**4**), 50.7 (**5**), 67.6 (**6**). (d) DOPC/SM/cholesterol (1:1:1), c_L = 118 nM; c_P/nM = 0 (**1**), 0.1 (**2**), 0.6 (**3**), 0.9 (**4**), 2.4 (**5**), 5.9 (**6**), 11.8 (**7**). Points from mixed protein−lipid isotherms corresponding to the Π−*A* combinations used for TM-AFM (Figures 3 and 4 and Figures S6−S9) and BAM studies (Figure 5) are shown as diamonds and triangles, respectively. Points used for BAM on lipid-only isotherms are indicated by asterisks.

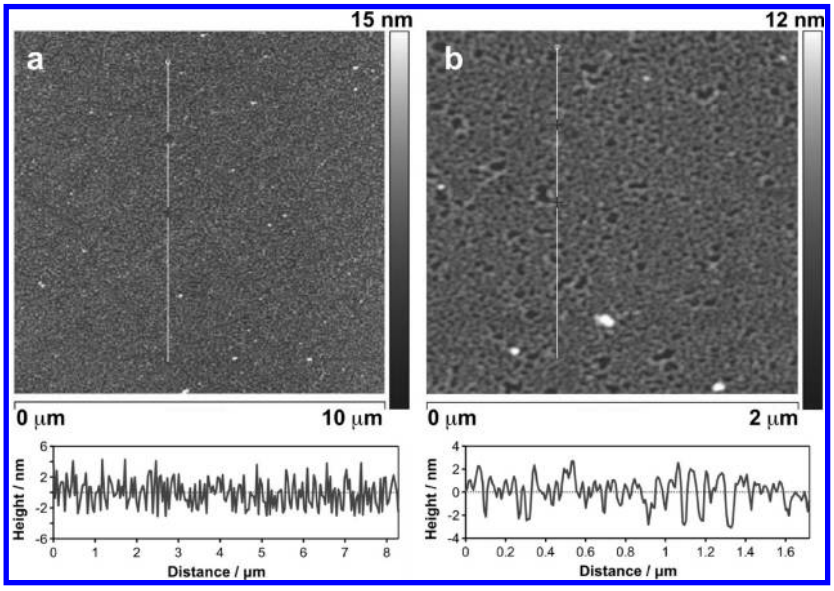

Figure 3. TM-AFM height images of surfaces prepared by transfer from monolayers of DOPC/DPPC/cholesterol (1:1:1, $c_L = 7.6 \times 10^{-8}$ M) and RSV M protein ($c_P = 3.8 \times 10^{-9}$ M), spread on PBS subphases at 20 °C and pH 7.4, to modified silicon substrates at Π = 29 mN m^{-1}. Surfaces correspond to the face of the monolayer in contact with the subphase.

to the protein concentration range. In the low concentration regime (e.g., c_P = 0.1 nM, isotherm 2), the protein exhibited simple partitioning to the interface in competition with the lipid.

At the limiting spreading pressure of the protein (Π^{max}, 12.7 ± 1.3 mN m^{-1}), the protein was expelled from the monolayer to leave a film of insoluble lipid, demonstrated by the convergence of the Π−*A* isotherms of the protein−lipid and lipid-only (c_P = 0, isotherm 1) monolayers at this pressure. At intermediate concentrations (e.g., c_P = 0.6 nM, isotherm 3), protein partitioning into the monolayer produced a marked transition at the limiting spreading pressure of the protein, demarcated by a corresponding plateau in the Π−*A* isotherm. More strikingly, isotherms in this intermediate concentration range crossed the lipid-only isotherm in the plateau region, resulting in smaller areas per lipid molecule than found for the lipid-only monolayer at surface pressures greater than 12.7 mN m^{-1}.

At higher concentrations (e.g., c_P = 6 nM, isotherm 6), saturation behavior was found, again with the occurrence of a transition

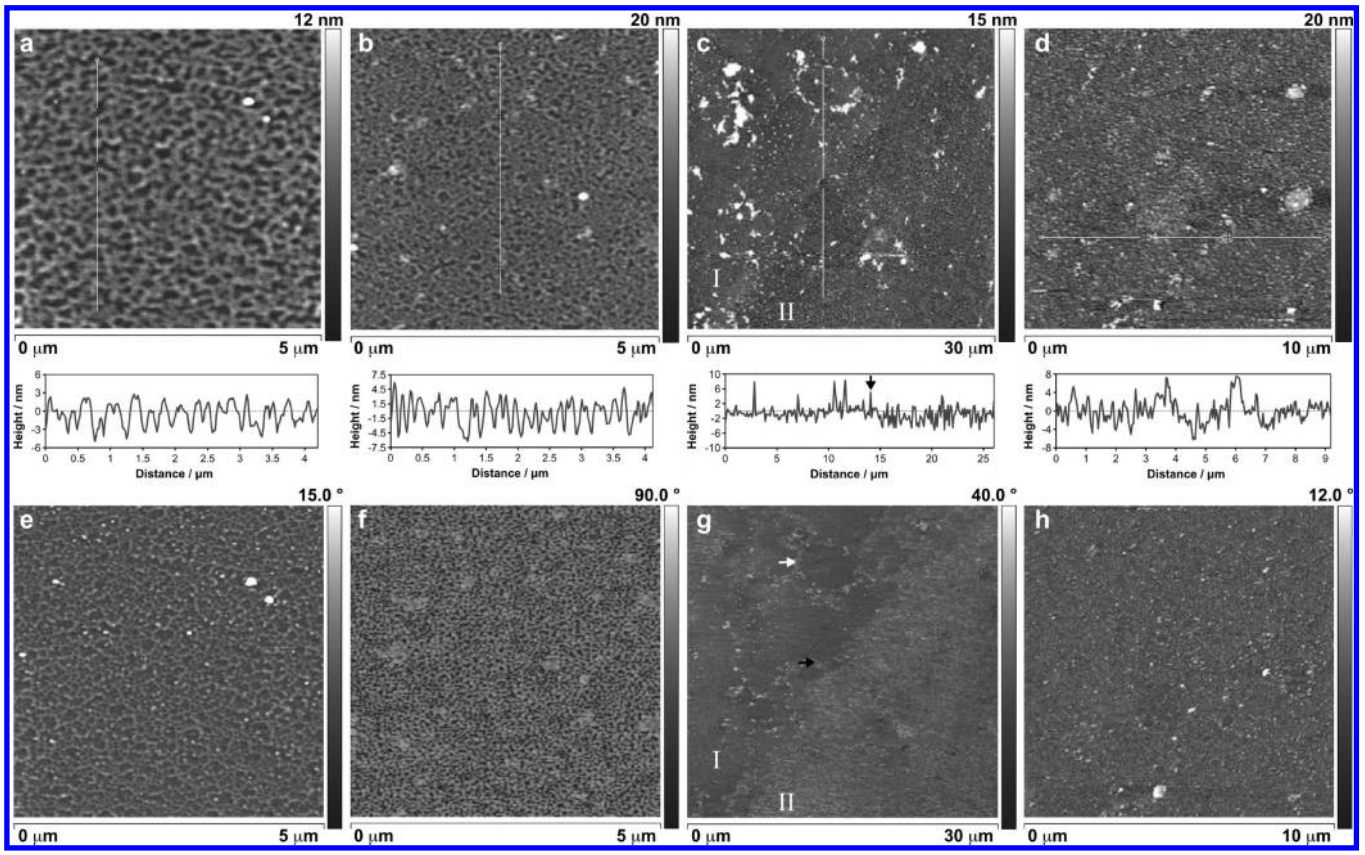

Figure 4. Tapping mode AFM images of surfaces prepared by transfer from monolayers of DOPC/SM/cholesterol (1:1:1, c_L = 77 nM) and RSV M protein (c_P = 0.8 nM), spread over PBS subphases at 20 °C and pH 7.4, to modified silicon substrates. Surfaces correspond to the face of the monolayer in contact with the subphase. Sections through the data are shown below the corresponding image. (a, b) Height scans following deposition at 8.8 mN m^{-1}. (c) Height scan at 8.8 mN m^{-1}. Two regions identified by "I" and "II" are evident. (d) Height scan following deposition at 17.3 mN m^{-1}. (e)−(h) Phase images corresponding to (a) to (d).

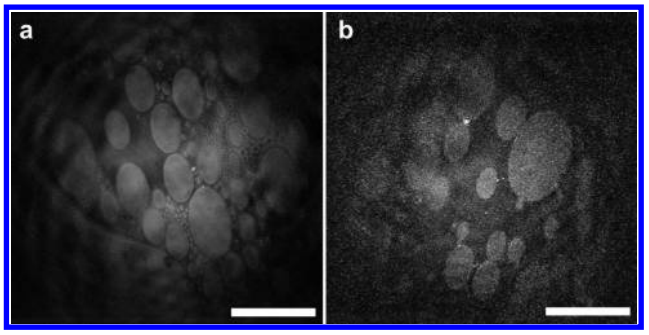

Figure 5. BAM images from compression isotherms of DOPC/SM/cholesterol monolayers (1:1:1, c_L = 178 nM) spread over PBS subphases at pH 7.4, 20 °C. Scale bars represent 500 μm in each case. Images are shown from (a) a lipid-only film (Π = 4 mN m^{-1}) and (b) a mixed lipid/RSV M (c_P = 3.8 nM) film (Π = 8 mN m^{-1}).

and corresponding plateau, in this case at Π = 16 mN m^{-1}. Isotherms in this protein concentration range similarly transected the lipid-only isotherm at surface pressures greater than 16 mN m^{-1}, again reflecting the formation of monolayers that were more condensed than those of the lipid in the absence of protein.

The reduction in area per lipid molecule for sphingomyelin-rich monolayers in the presence of RSV M protein at surface pressures greater than Π^{max} indicated that either significant material, including lipids, was being lost from the interface by desorption at these surface pressures or peripheral association of the protein with the monolayer was occurring in a manner that favored the formation of a more condensed interfacial layer. Using a higher concentration of lipid (Figure S5), it was possible to compress the monolayer to the point of collapse, at a surface pressure of 72 mN m^{-1}. The area per lipid molecule at the collapse pressure was similar (49 Å^2) in the presence or absence of protein. The similarity of the collapse areas and pressures of these monolayers, formed either with our without RSV M, indicates that neither collapse of the film nor loss of lipidic material from the interface occurs in the plateau region. Therefore, in order to augment the $\Pi-A$ data and confirm that protein association with the surface of the lipid film was occurring at higher pressures in the presence of SM, the protein topology at the interface and the mixing behavior with lipids were investigated using atomic force microscopy (AFM) and Brewster angle microscopy (BAM), respectively.

Surface Topography of M−Lipid Monolayers. Mixed protein−lipid films were deposited at constant pressure onto oxidized silicon surfaces that had been silanized by treatment with octadecyltrichlorosilane.[40] Surface pressures were selected to represent the key sections of the isotherms, with film deposition conducted in a manner that permitted the face of the monolayer in contact with the subphase to be examined by tapping mode atomic force microscopy (TM-AFM). Prior to deposition, the protein was fixed by a glutaraldehyde treatment to ensure film stability. Without fixing, films (including those of lipids in the absence of protein) were not sufficiently stable to allow imaging. In the case of DOPC/DPPC/cholesterol/M, deposition at 29 mN m^{-1} produced surfaces characterized by a relatively low

(40) Watson, S. M. D.; Coleman, K. S.; Chakraborty, A. K. *ACS Nano* **2008**, *2*, 643–650.

roughness (R_q = 1.0 ± 0.1 nm, R_a = 0.8 ± 0.1 nm) and uniform dispersion of material, evident in both height (Figure 3a) and phase (Figure S6) imaging modes.

As this deposition pressure is in the same region of the isotherm as the monolayer−bilayer equivalence pressure (35 mN m^{-1}),[39] it is therefore representative of the interface at the latter pressure. Pinhole defects are frequently observed in Langmuir−Blodgett films of this type when imaged at high-resolution by AFM;[41] such defects were detected in higher resolution images of the film (Figure 3b), enabling the depth of the film to be measured, yielding a value of 3.3 ± 1.6 nm.

Films were deposited from DOPC/SM/cholesterol/M monolayers at surface pressures above and below the transition and corresponding plateau in the Π−*A* isotherm. At a pressure of 8.8 mN m^{-1}, below Π^{max}, two types of surface texture were distinguishable. The first (Figure 4a,e) was characterized by an even distribution of surface features that had a similar depth profile (4.0 ± 1.1 nm) to DOPC/DPPC/cholesterol/M films, albeit with a rougher texture (R_q = 1.7 ± 0.2 nm, R_a = 1.4 ± 0.1 nm). The second (Figure 4b,f) had a denser surface coverage, a rougher texture (R_q = 2.1 ± 0.3 nm, R_a = 1.7 ± 0.2 nm), and a more profound depth profile, with features of height 6.5 ± 2.5 nm. More strikingly, phase images of the second regions were considerably more uniform (Figure 4f), revealing a significantly higher density of material at the surface than apparent from the corresponding height images (Figure 4b).

The two distinct surface textures were similarly apparent in lower resolution scans, particularly from phase images (Figure 4c,g; regions labeled I and II). Although the surface in Figure 4c is more disordered than those of Figure 4a,b, a height difference of ∼3 nm exists between the two regions, which is consistent with the difference in feature depths observed in Figure 4a,b. The more densely covered region (region I) additionally contains circular features (indicated by a white arrow in Figure 4g). These circular features are surrounded by material of raised profile, but similar viscoelastic properties to the material in region II, suggesting that the raised areas are material that has been expelled by annealing during surface compression, consistent with the formation of these regions by annealing of separate microdomains on the surface.

Films deposited from DOPC/SM/cholesterol/M at 17 mN m^{-1}, above Π^{max}, produced surfaces of consistently rough texture (R_q = 2.8 ± 0.4 nm, R_a = 2.2 ± 0.3 nm; Figure 4d and Figure S7) with no pinhole defects. Some heterogeneous areas were detected on the surface, with features in these areas of height 5−10 nm, indicating a significant change in surface properties at these pressures.

Brewster Angle Microscopy (BAM). BAM is sensitive to changes in refractive index at the air−water interface and is consequently a useful technique for observing microscopic changes in surface properties, such as mixing or separation of monolayer components, without the need for introducing artificial labels that may perturb surface equilibria. BAM was conducted on DOPC/DPPC/cholesterol and DOPC/SM/cholesterol films in order to ascertain the mixing behavior of these lipids in the presence of RSV M protein. Films of DOPC/DPPC/cholesterol yielded no evidence of inhomogeneity at pressures below 60 mN m^{-1}, irrespective of the presence or absence of the protein (Figure S8). Although this mixture of lipids exhibits microphase separation, l_0 domains in this mixture are generally submicrometer in diameter,[31] so the lack of surface texture is not surprising. However, the data do illustrate that there is no significant phase separation, at least on a microscopic scale, in the presence of protein. At surface pressures corresponding to film collapse, extensive formation of highly condensed phases occurred within a few minutes, leading eventually to the observation of insoluble material in the field of view (Figure S8c), consistent with film collapse at these pressures.

Films of DOPC/SM/cholesterol revealed a more complex behavior. At low pressures in the absence of protein, a mixture of fluid (dark, l_0) and more condensed (light, l_d) phases was observed, with the latter comprising circular domains of diameter 20−100 μm (Figure 5a). Features of this size were anticipated at 20 °C, considering the documented formation elsewhere of large liquid-ordered domains with this ternary lipid mixture.[29]

As the surface pressure was increased, these domains become smaller, but of higher contrast (Figure S9a). In the presence of RSV M, at low pressures (below Π^{max}) the circular condensed-phase domains persisted (Figure 5b), although there was a slight increase in both the diameter and roughness of the edges. As the pressure was increased to 13 mN m^{-1}, in the plateau region of the isotherm ($\approx\Pi^{max}$), more uniform textures were formed (Figure S9b). These data indicate that l_d domains, present both at low surface pressures and pressures close to Π^{max}, are not disrupted by the protein and may in fact be stabilized to a small degree.

Protein Assembly. RSV M protein was incubated with each lipid mixture in order to investigate the potential for ordered structures to form over extended time periods. Because of the impracticality of conducting experiments lasting several days on thin films, these experiments were conducted by adding protein solutions to thin films of lipid adsorbed on a glass surface. In the majority of cases no evidence was obtained for ordered protein assembly. However, in the case of DOPC/DPPE, extensive assemblies several micrometers in length and of uniform diameter were found (Figure 6a).

Although the most regular assemblies were formed with the His-tagged protein, it was possible to prepare similar assemblies from the untagged protein (Figure 6b). In order to separate these assemblies from excess protein and lipid, sucrose flotation experiments were conducted.

Samples from low-density lipoprotein fractions contained clear evidence for ordered assembly of the protein into a helical array of diameter 29 nm and pitch 33 nm (Figure 6c). From the observation of nascent assemblies extending from the surface of spherical objects resembling liposomes (Figure 6d), it is apparent that the lipid is a key requirement for their formation. The formation of these assemblies was also observed, albeit less frequently, with DOPC/SM/cholesterol mixtures (Figure 7).

Discussion

The aim of this work, in the absence of data on the distribution of lipids in the viral envelope, was to use model lipid monolayers at the air−water interface to determine whether the RSV M protein is able to interact with specific lipid components of the envelope. To this end, the Π−*A* data provide the key evidence that the nature of the protein adsorption is dependent on the lipid composition of the monolayer, in particular the presence or absence of sphingomyelin. For monolayers composed of DOPC, DOPC/DPPE, or DOPC/DPPC/cholesterol, it is clear from the significant pressure and area increases produced by protein partitioning to the interface, over the whole range of pressures below film collapse, that the RSV M protein inserts between lipid molecules and penetrates the monolayer. The protein remains adsorbed at the interface beyond its limiting surface pressure (Π^{max}) of 12.7 mN m^{-1} and well beyond the monolayer−bilayer equivalence pressure of 35 mN m^{-1},[39] which is representative of the

(41) Schwartz, D. K. *Surf. Sci. Rep.* **1997**, *27*, 245–334.

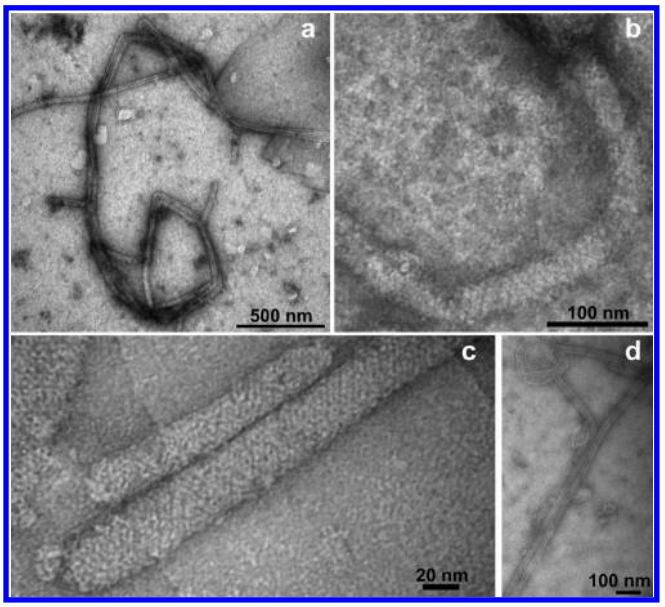

Figure 6. Negative stain (uranyl acetate) transmission electron micrographs of structures formed following incubation of RSV M protein with DPPE/DOPC (1:4). (a) Initial preparation with His-tagged M (c_P = 34 μM, c_L = 87 μM). (b) Preparation with untagged protein (c_P = 17 μM, c_L = 44 μM). (c) The sample from (a) following enrichment by sucrose flotation, showing a helical assembly of diameter 29 nm and pitch 33 nm. (d) Nascent assemblies extending from the surface of a liposome.

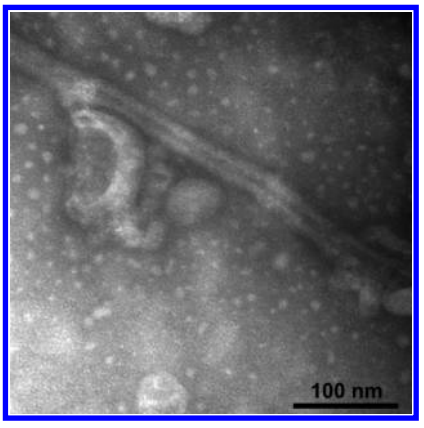

Figure 7. Negative stain (uranyl acetate) electron micrographs of tubules formed following incubation of RSV M with DOPC/SM/cholesterol (1:1:1), c_P = 47 μM, c_L = 0.2 mM.

surface pressure in cell membranes and a useful reference point for *in vivo* activity. It is also notable that saturation of the monolayer occurs at protein concentrations that are only slightly higher (but of the same order of magnitude) than the concentration (c_P^{max}) at which saturation of the interface by protein occurs in the absence of lipid. The low saturation concentrations and the stability of the film beyond Π^{max} indicate that lateral protein−lipid interactions contribute to protein adsorption in these cases.

For monolayers composed of DOPC/SM/cholesterol, the behavior of the protein below Π^{max} in $\Pi-A$ isotherms is the same as that observed for monolayers without SM; that is, penetration of the monolayer occurs up to a saturating protein concentration that is of the same order of magnitude as c_P^{max}. In this case, however, at a surface pressure corresponding to Π^{max}, the protein is expelled from the interface. For higher protein concentrations, at surface pressures greater than Π^{max}, the film assumes a smaller area per lipid molecule in the presence of protein than the lipid-only monolayer. Of the two potential scenarios that could lead to this reduction in area, namely loss of lipid material from the monolayer or adsorption of the protein to the surface, the latter has been shown to operate due to the similar collapse area and pressure films formed in the presence and absence of protein.

While the TM-AFM and BAM data are not, by themselves, sufficient to reach conclusions on the behavior of the protein, they nevertheless provide useful evidence in support of the findings arising from analysis of the $\Pi-A$ isotherms. In the case of TM-AFM imaging of protein films, some sample artifacts are likely to be introduced during sample preparation, although different protein dispositions in the monolayers should still be reflected by differences in the material properties of the films once deposited. In this regard, the AFM images support the $\Pi-A$ analysis in that areas of film of similar surface texture are obtained by deposition from DOPC/DPPC/cholesterol monolayers and DOPC/SMcholesterol monolayers below Π^{max} (both sets of conditions being characterized in $\Pi-A$ isotherms by protein penetration of the monolayer). In the case of DOPC/SM/cholesterol, a second region of these films can be distinguished with different material properties. It is noteworthy that the surface features in these areas are deeper by approximately 2.5−3 nm than those associated with penetrated protein. Some of this depth increase is attributed to the protein itself, with the remainder arising from the greater height (by ∼1 nm) of l_0 domains when compared with l_d domains.[42] For DOPC/SM/cholesterol at surface deposition pressures greater than Π^{max}, a new film texture is found, characterized by a greater roughness, greater feature depth, and more dense surface coverage. These are exactly the features expected for a peripheral dispostion of the protein, supporting the assignment made by analysis of the $\Pi-A$ isotherms.

In the case of BAM data, the spatial resolution is limited (at best) to the diffraction limit, and as a consequence, inhomogeneity on length scales shorter than this will not be resolvable. Nevertheless, it was possible to exploit the formation of large l_0 domains by DOPC/SM/cholesterol mixtures to determine whether the protein perturbed domain formation in this system. The small changes in the morphology of the domains observable by BAM with and without protein indicates that domain formation not disrupted by the protein at pressures below Π^{max}. Peripheral association to SM-rich domains has been demonstrated for the peptide equinatoxin; in this case, association additionally occurred with the boundary of l_0 domains, leading to the formation of blebs.[43] This cannot be ruled out in this case, particularly at pressures greater than Π^{max}.

Given that DOPC/DPPC/cholesterol mixtures are known to form l_0 phases,[26−28] the data point to the presence of specific interactions with SM, rather than binding to l_0 domains *per se*, as the reason for peripheral binding to DOPC/SM/cholesterol monolyers. Up to 10% of the total SM is expected to reside in the l_d phase,[44] which is sufficient to account for expulsion of the protein from this phase as the area of the monolayer is reduced and the density of SM sites increases. The changes to the isotherms that occur as the protein concentration is varied are rationalized by corresponding changes to the relative occupancy of the available adsorption sites in the l_0 and l_d phases in the different concentration regimes.

(42) Keating, E.; Rahman, L.; Francis, J.; Petersen, A.; Possmayer, F.; Veldhuizen, R.; Petersen, N. O. *Biophys. J.* **2007**, *93*, 1391–1401.
(43) Alison Drechsler, A.; Anderluh, G.; Norton, R. S.; Separovic, F. *Biochim. Biophys. Acta* **2010**, *1798*, 244–251.
(44) Wang, T. Y.; Silvius, J. R. *Biophys. J.* **2003**, *84*, 367–378.

Association of RSV M with the membrane has been shown to involve contributions from both electrostatic interactions and hydrophobic effects.[45] The crystal structure of the protein (Figure S3) is delineated by the presence of two domains, with hydrophobic surfaces sequestered at the interface between the domains and a signficant positively charged patch extending over the surface of the protein.[33] As the monolayer experiments were conducted with neutral lipids, hydrophobic effects could be expected to play a significant role in determining surface partitioning, which accounts for the area per protein molecule at the surface, as movement of the two domains is required to expose the hydrophobic surface. However, electrostatic interactions with SM are the only effective means for accounting for the behavior of the protein in monolayers containing this lipid.

Incubation of RSV M with lipid mixtures over periods of several days demonstrated an inherent propensity of the protein to self-assemble to form helical arrays. Interestingly, helical striations are observed by EM following removal of the envelope from RSV filaments by freeze fracture,[5] which indicates that a similar self-assembly process occurs *in vivo*. The same study reports the formation of filamentous virions several micrometers in length, which is consistent with the length scales we observe for M protein assembly. On the basis of our $\Pi - A$ data, it is clear that this assembly occurs from protein that is integral to the membrane rather than peripherally bound. It has been suggested that cholesterol is a key requirement for the formation of filaments,[46] which is not inconsistent with our data given that monolayer penetration by the protein occurs in the presence of cholesterol.

(45) Harrison, M. S.; Sakaguchi, T.; Schmitt, A. P. *Int. J. Biochem. Cell Biol.* **2010**, *42*, 1416–1429.

(46) Yeo, D. S.; Chan, R.; Brown, G.; Ying, L.; Sutejo, R.; Aitken, J.; Tan, B.; Wenk, M. R.; Sugrue, R. J. *Virology* **2009**, *386*, 168–182.

Conclusions

The key conclusion from this work is that, at physiologically relevant surface pressures, the RSV M protein penetrates membranes deficient in sphingomyelin and associates peripherally (extrinsically) with membranes rich in sphingomyelin. From this it is evident that the membrane-associative behavior of the protein is dependent on, and influenced by, changes in membrane lipid composition. As the detailed distributions of lipids are poorly characterized for both the viral envelope, and the plasma membrane of the diseased cell prior to virion release, these data are valuable for our understanding of M protein activity.

Acknowledgment. The authors thank Sarah Keller for advice during the preparation of this manuscript and Christine Richardson for technical assistance. The work was supported by contributions from Durham University, OneNorthEast, and the Wolfson Research Institute.

Supporting Information Available: Full experimental methods, additional figures (BAM, AFM, and EM), and additional isotherms. This material is available free of charge via the internet at http://pubs.acs.org.